



Study on cutting performance of SiCp/Al composite using textured YG8 carbide tool

Xu Wang^{1,2} · Valentin L. Popov^{1,2} · Zhanjiang Yu¹ · Yiquan Li¹ · Jinkai Xu¹ · Huadong Yu¹

Received: 17 June 2021 / Accepted: 5 November 2021
© The Author(s) 2021

Abstract

Precision machining of SiCp/Al composites is a challenge due to the existence of reinforcement phase in this material. This work focuses on the study of the textured tools' cutting performance on SiCp/Al composite, as well as the comparison with non-textured tools. The results show that the micro-pit textured tool can reduce the cutting force by 5–13% and cutting length by 9–39%. Compared with non-textured tools, the cutting stability of the micro-pit textured tools is better. It is found that the surface roughness is the smallest (0.4 μm) when the texture spacing is 100 μm , and the residual stress can be minimized to around 15 MPa in the case of texture spacing 80 μm . In addition, the SiC particles with size of around 2–12 μm in the SiCp/Al composite may play a supporting role between the texture and the chips, which results in three-body friction, thereby reducing tool wear, sticking, and secondary cutting phenomenon. At the same time, some SiC particles enter into the micro-pit texture, so that the number of residual particles on the surface is reduced and the friction between the tool and the surface then decreases, which improves the surface roughness, and reduces the surface residual stress.

Keywords SiCp/Al composite · Micro-textured tool · Secondary cutting

1 Introduction

The SiCp/Al composite material is mainly composed of aluminum alloy as the matrix and SiC particles as the reinforcing phase. Due to its special physical properties, including high hardness, low thermal expansion coefficient, high thermal conductivity, and high wear resistance, it has been widely used in aerospace, automotive, electronics, medical, optical instruments, and other fields [1–6]. The cutting process of SiCp/Al composite is quite complicated. Due to the large elastoplasticity of the aluminum matrix and the high hardness of SiC particles, the tool is very quickly worn. Liu et al. [7] studied the influence of the position of the tool and the SiC particles on the cutting performance in the processing of SiCp/Al composites, and found that when the tool was

located at a lower position in the middle of the SiC particles, the stress turned to greater, which can cause the entire SiC particles to break. Niu and Cheng [8] conducted milling experiments on SiCp/Al composites. During the machining process, although the plastic deformation of the aluminum matrix can fill part of the pits caused by the SiC particles on the surface of the workpiece, there are still some defects on the surface. For a better application of the SiCp/Al composite under a harsh working condition, it is important to study on its machining method [9].

A large number of experiments and theoretical explorations on the cutting performance of micro-textured tools and the lubrication performance of the surface have been conducted. Liu et al. [10] produced different textures on the flank face of cemented carbide tools, and further studied the wear resistance and machining surface quality of micro-textured tools. They found that the flank face of the tool with textures is more excellent in terms of the wear resistance and surface machining quality. The parameters with good cutting performance are as follows: the groove width is 75 μm , the groove spacing is 100 μm , and the distance between the groove and the main cutting edge is 75 μm . Zhang et al. [11] prepared a sinusoidal groove micro-texture on the surface of cemented carbide using laser technology.

✉ Valentin L. Popov
v.popov@tu-berlin.de

✉ Zhanjiang Yu
13514310244@163.com

¹ National and Local Joint Engineering Laboratory for Precision Manufacturing and Detection Technology, Changchun University of Science and Technology, Changchun 130012, Jilin, People's Republic of China

² Technische Universität Berlin, 10623 Berlin, Germany

They performed a linear reciprocating friction and wear test on the textured surface. The results showed that the surface of the sinusoidal micro-textured sample had the best wear resistance under the conditions of high load, high sliding speed under the condition of adding grease. Wu et al. [12] simulated the cutting process of micro-textured tool cutting Ti-6Al-4 V alloy using the finite element method, and carried out experimental verification. The results showed that micro-textured tools can reduce cutting temperature, cutting force, and tool-chip contact length. And it is easier to break the chips with the micro-textured tool. In addition, compared with the rectangular cross-section groove, the V-shaped cross-section groove can reduce the severity of secondary cutting.

In addition, Zheng et al. studied the cutting performance of micro-textured tools for cutting Ti-6Al-4 V titanium alloy [13]. They selected YG8 tools and studied the cutting performance with four types of textured tools, namely, non-textured tools, line textured tools, sinusoidal textured tools, and rhombic textured tools. Among them, the groove width of the micro-textured tool is 159.599 μm and the groove depth is 14.59 μm . It was found that the sinusoidal textured tool has the best cutting effect under different cutting parameters. It can reduce the cutting force and surface roughness, and extend the tool life. Feng et al. [14, 15] conducted cutting experiments on AISI 1045 steel based on micro-textured tools with transverse micro-texture morphology. The texture structure is as follows: 0.2 mm from the main cutting edge, 0.1 mm spacing, 0.1 mm width, and 0.1 mm depth. By designing positions, spacings, and widths of textures, the tool was finally obtained the best cutting performance. They found that the secondary cutting phenomenon is not obvious with the increasing groove width. The width of the groove and the cutting speed are the key factors that affect the secondary cutting during the machining. The measurement of cutting force, cutting temperature, workpiece surface roughness, and tool wear showed that compared with traditional tools, textured tools reduced cutting force, cutting temperature, tool wear significantly, and improved workpiece roughness. Vasumathy and Meena [16] studied the friction and adhesion of the tool-chip interface of AISI316 austenitic stainless steel during the machining. They found that the micro-textured tool can reduce the adhesion of the tool-chip, cutting force, and minimize the friction between the tool-chip interface. In order to study the effect of surface texture on Si₃N₄/TiC ceramics, Xing et al. [17, 18] prepared regularly arranged micro-grooves on the surface of Si₃N₄/TiC ceramics using a laser. It was showed that compared with the smooth surface, the textured surface can reduce the friction coefficient and improve the wear resistance of the material. And the tribological properties depend on the size and spacing of the micro grooves largely. To improve the friction and anti-adhesion of the

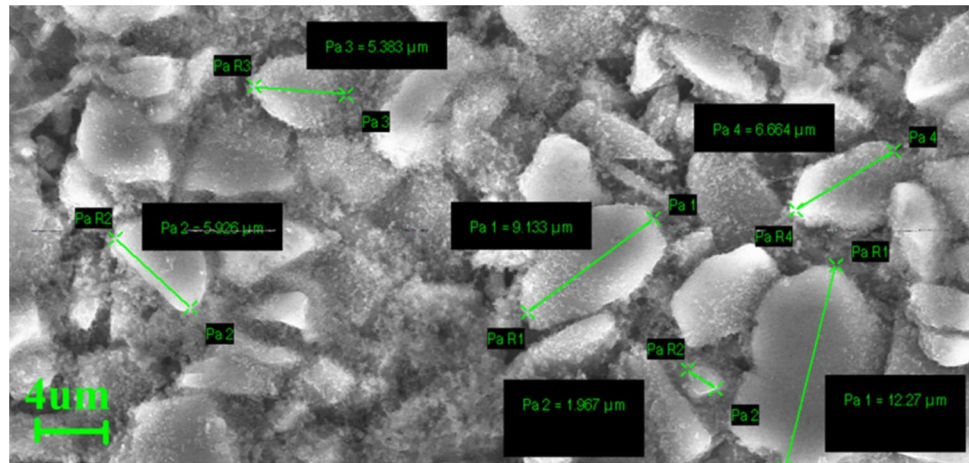
tool rake face in the dry cutting of aluminum alloy, three textures on the cemented carbide rake face were created. It was found that the texture geometry has the greatest influence on the cutting force and friction coefficient in the cutting performance. Parida et al. [19] evaluated the cutting performance of Ti-6Al-4 V alloy micro-textured tools experimentally and numerically. The results showed that the contact length, friction coefficient, cutting force, and tool temperature distribution of the chip and the micro-textured tool were significantly reduced, compared with the flat tool. The cutting force, chip reduction coefficient, and chip morphology in the square result were consistent with the experimental results well. Sivaiah et al. [20] conducted a study on the cutting performance of the hybrid-textured tool and found that the friction between the textured tool and the chip was significantly reduced under wet cutting conditions, and the machined surface roughness was quite small. Elias et al. [21] proposed a new method to make texture on the cutting tools using vickers microhardness indenter.

Traditional cutting tools would produce large cutting forces and strong tool wear during machining [22, 23]. There are very few studies on the machining of SiCp/Al composite using textured tools. In this work, the machining experiments of SiCp/Al composite will be performed to investigate the cutting performance of SiCp/Al composite with comparison to that of the non-textured tool. By preparing very small pits (about 5 μm in diameter and 30 μm in depth), the cutting performance of the tool and the surface quality of the workpiece will be studied. The influence of spacing on the cutting performance of micro-pit array textured tool will be investigated. The secondary cutting phenomenon will be observed, and the surface properties of the workpiece will be analyzed during the machining of SiCp/Al composite to obtain the optimal texture parameters of the tool.

2 Materials and methods

The surface of the SiCp/Al composite after grinding and polishing is shown in Fig. 1. It can be seen that the SiCp/Al composite is composed of an aluminum matrix and SiC particles. Due to the greater plasticity of the aluminum matrix and the high hardness of SiC particles, the aluminum matrix is removed during the polishing process, and the silicon carbide particles are exposed on the surface of the material. By measuring the SiC particles by the SEM, it is found that the size of the smallest SiC particles is about 2 μm , and the large SiC particles can reach about 12 μm . Moreover, some particles are pulled out and broken during the machining, which might interact with the textured tool and makes the micro-textured tool cutting process more complicated. This is completely different from the cutting of traditional metal

Fig. 1 Image of SiCp/Al composite structure after grinding and polishing under the SEM



materials. The high hardness of SiC particles makes the tool wear very quickly and strong during the machining. The micro-textured tools cutting SiCp/Al composite is studied in the following.

The micro-cutting experiment setup was developed which can be used to perform orthogonal cutting experiment, as shown in Fig. 2a. Figure 2b gives a schematic diagram of the cutting process. The overall size of the orthogonal cutting table is $300 \times 400 \times 300$ mm, and size of the X and Y slide table is 70×110 mm. The stroke of slid table is 50 mm, and its positioning accuracy is 2 μ m, the repeated positioning accuracy is 0.5 μ m, and the maximum feed speed is 400 mm/s. The size of the Z-direction lifting slide is 120×120 mm, the maximum ascent stroke is 12 mm, the repeated positioning accuracy is 0.5 μ m, and the bearing capacity is 20 kg. The cutting force is measured by the Kistler cutting force measuring instrument.

In the experiment, the uncoated cemented carbide tool (NTK-KM1CCGW060202H) was used for machining. The rake angle is 7° , the flank angle is 3° , and a cutting-edge radius is 2 μ m. Nanosecond pulsed fiber laser is used to manufacture the micro-pit texture on the rake face near the main cutting edge. The laser wavelength is 1.064 μ m, the maximum output power is 20 W, and the pulse frequency is 20–200 kHz.

The textured pits are as shown in Fig. 3. The pits are regularly distributed on the rake surface with different spacings. In this work, five values of pits spacing are investigated as follows: 100 μ m, 80 μ m, 60 μ m, 40 μ m, and 20 μ m. The other parameters are as follows. The diameter of the pit is around 5 μ m (green circle in Fig. 3a); the depth is around 30 μ m (Fig. 3b). The distance between the

texture and the cutting edge is around 20 μ m (Fig. 3c). The workpiece size is $10 \times 10 \times 1$ mm (cutting width 1 mm), the cutting speed is set constant with 400 mm/s, the cutting depth is around 30 μ m, and the cutting repeats 10 times. Table 1 numbers the textured tools with different pit spacing and the workpieces processed by different textured tools.

3 Results and discussion

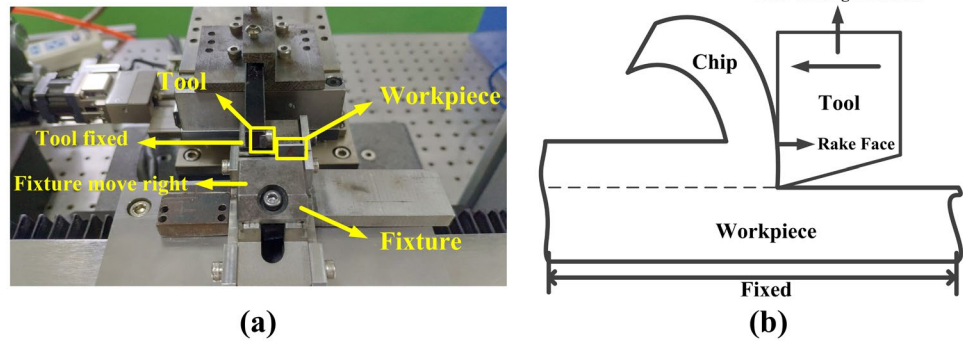
Based on the experimental results, the wear of tool, contact length, secondary cutting, cutting force, and surface quality of workpieces were analyzed.

The surface of the tools was observed and inspected using a scanning electron microscope (SEM) after 10 cuttings. Figure 4a shows the surface of non-textured tool (T-1) after 10 cuttings, and Fig. 4b–f that of micro-textured tools with different spacing from 100 to 20 μ m. It can be evaluated that the wear of tools and tool-chip adhesion are very serious during machining SiCp/Al composite material. Among these six tools, the non-textured tool is worn most near the tool edge. Moreover, the amount of chip sticking on the surface of the non-textured tool is also the largest. It can be clearly seen from Fig. 4b–f that the micro-textured tool reduces not only tool wear during machining, but also the adhesion of tool surface effectively. The reduction of tool wear can be mainly attributed to the pit array which decreases the contact area and state between the tool and chip during the cutting process, thereby reduces the friction as well as the tool wear. The decrease in surface adhesion of the tool may be due to the effect of pits and SiC particles on chips during

Table 1 Numbers of tools and workpieces

Tool number	T-1	T-2	T-3	T-4	T-5	T-6
Texture spacing	Non-textured	100 μ m	80 μ m	60 μ m	40 μ m	20 μ m
Workpiece number	W-1	W-2	W-3	W-4	W-5	W-6

Fig. 2 (a) Orthogonal cutting experiment table. (b) Schematic diagram of machining



the cutting process. Observing Fig. 4e, it can be seen that the surface of the tool with a pit spacing of $40\text{ }\mu\text{m}$ has very small amount of adhesion, and there is no adhesion around the micro-pit at the edge of the tool. Although some pits are blocked, the micro-pit array still plays an important role in reducing the adhesion condition of the cutting tool and chips.

Another reason for the reduction of tool surface adhesion may be due to the fact that some SiC particles play a supporting role between the tool and the chips, thereby reducing the direct contact between the tool and the chips. The adhesion phenomenon on the surface of the textured tool has been reduced in different ways, and the T-5 tool is the most obvious. When the texture spacing increases from 40 to $100\text{ }\mu\text{m}$, the anti-adhesion of the tool decreases. The main reason is that the texture area is reduced for large texture spacing; therefore, there is less texture interacting with chips. In the case of the texture spacing $20\text{ }\mu\text{m}$, the texture is too dense, which leads to an increase in the concentrated stress on the surface of the chip, as well as an increase in the surface adhesion of the textured tool.

For that, the energy spectrum analysis of the sticking area on the surface of the micro-textured tool was carried out. As shown in Fig. 5, in addition to the elements of the tool material, the selected elements and the remaining elements are Al and Si. From the distribution of Si, it seems that some of the smaller SiC particles enter into the pit or attach on the surface of the micro-textured tool during the cutting process,

then the SiC particles interact with the chip, which reduces the direct contact between the chip and the tool, resulting in a decrease in the adhesion on the surface of the micro-textured tool.

3.1 Contact length

The tool-chip contact length of T-1 to T-6 tools during the cutting process is shown in Fig. 6. The distance between the position with the highest tool wear and the main cutting edge is selected as the tool-chip contact length. It can be seen that the micro-textured tool can reduce the tool-chip contact length compared to the non-textured tool. The contact length is reduced by 39%, 22%, 30%, 32%, and 9% for T-2 to T-6 tools, respectively. The results show that the contact length for T-2 to T-5 tools is reduced significantly, and for T-2 tool, it is the smallest. During the machining of non-textured tools, the chips will break when they reach a wear state. However, the secondary cutting accelerates the chip's fracture. After the main cutting edge is machined, the micro-texture acts on the chip once again, which causes the breaking of chip before reaching the previous contact length. The texture changes the contact state of the bonding area. What actually changes is the curvature of the chips, which further affects the contact length between the chips. The main reason for the reduction in cutting length is that the texture will produce secondary cutting during the cutting process.

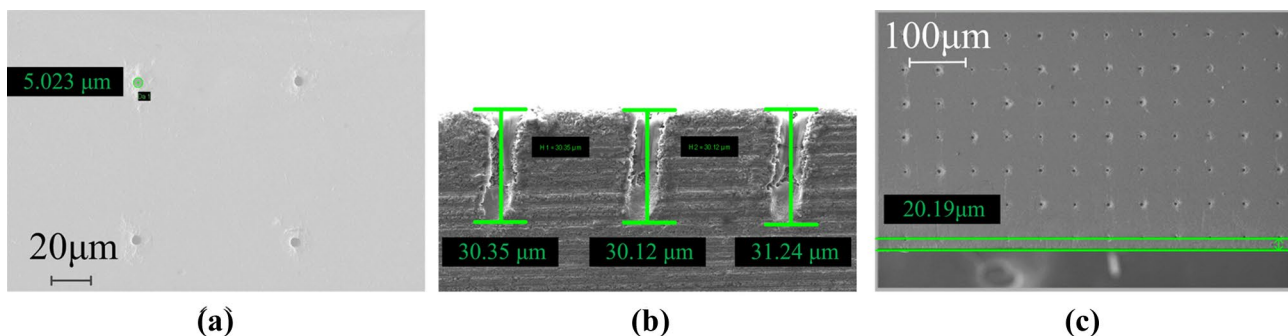


Fig. 3 (a) Top view of micro-textured pit diameter. (b) Profile of pit depth. (c) Distance between the micro texture and the main cutting edge

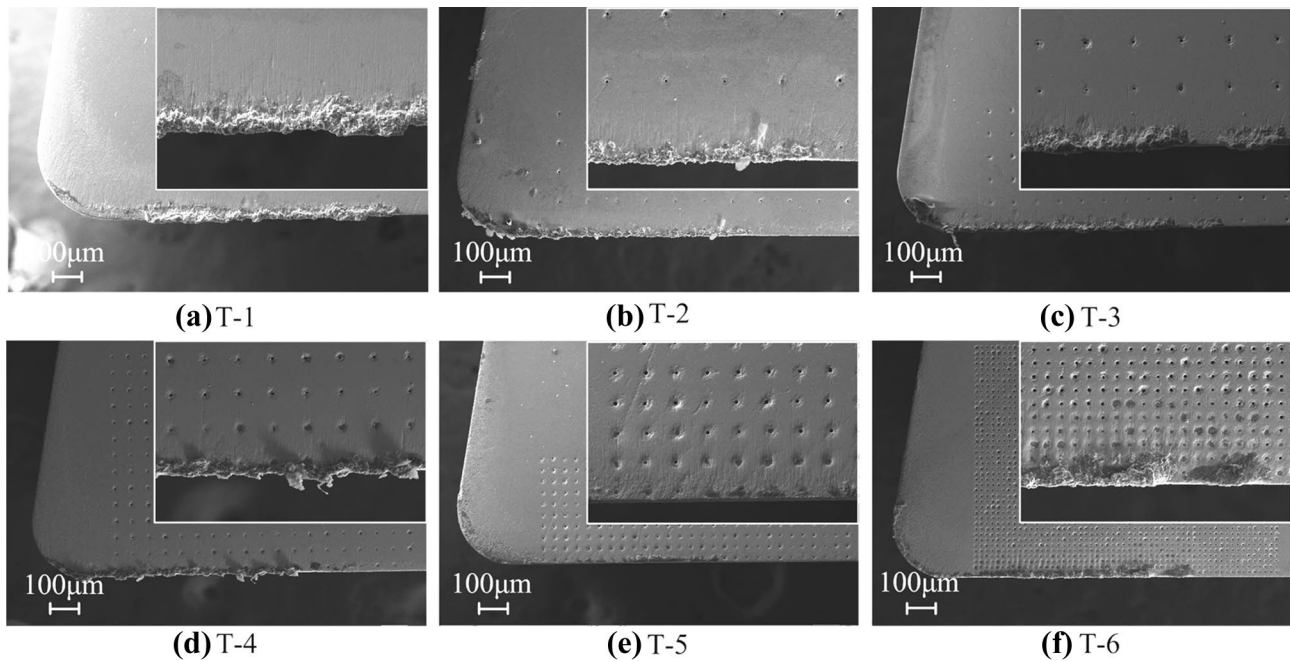


Fig. 4 SEM images of surfaces of non-textured and micro-textured tools after ten cuttings: (a) non-textured tools, (b) micro-textured tools with a pit spacing of 100 μm , (c) 80 μm , (d) 60 μm , (e) 40 μm , and (f) 20 μm

3.2 Secondary cutting

Secondary cutting is a common phenomenon in the cutting process of micro-textured tools. Comparing the chip surface micro morphology of Fig. 7a–f, it can be found that the chip surface machined by the textured tool will have textures with equal spacing. Therefore, it can be explained that the secondary cutting phenomenon will also occur in the process of machining SiCp/Al composite. However, this phenomenon is not so obvious as for traditional metal. The main disadvantage of secondary cutting is that the chips will be cut again

and new chips will be generated, leading to reducing the effectiveness of the micro-texture. From Fig. 7b–f, it can be seen that with the decrease of the micro-texture spacing, the phenomenon of secondary cutting becomes more obvious, which shows that too small texture spacing will increase the interaction between texture and chips. From Fig. 7c, e, T-3 and T-5 tools are more likely to break the chips during the cutting process, and then produce new chips. The secondary cutting phenomenon of T-2 and T-4 tools is not obvious

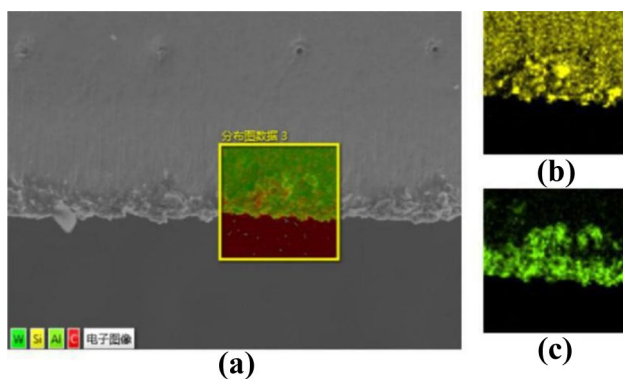


Fig. 5 (a) Energy spectrum analysis of micro-textured tool surface distribution of elements on the surface of micro-textured tools' edge. (b) Distribution of Al elements on the surface of micro-textured tools' edge. (c) Distribution of Si elements on the surface of micro-textured tools' edge

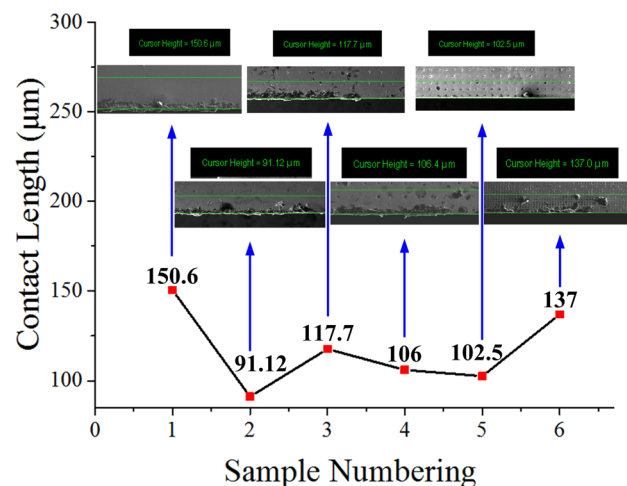


Fig. 6 Tool-chip contact length during the cutting process of non-textured tool and micro-textured tool. Numbering 1–6 corresponds to Tool T-1 to T-6, respectively

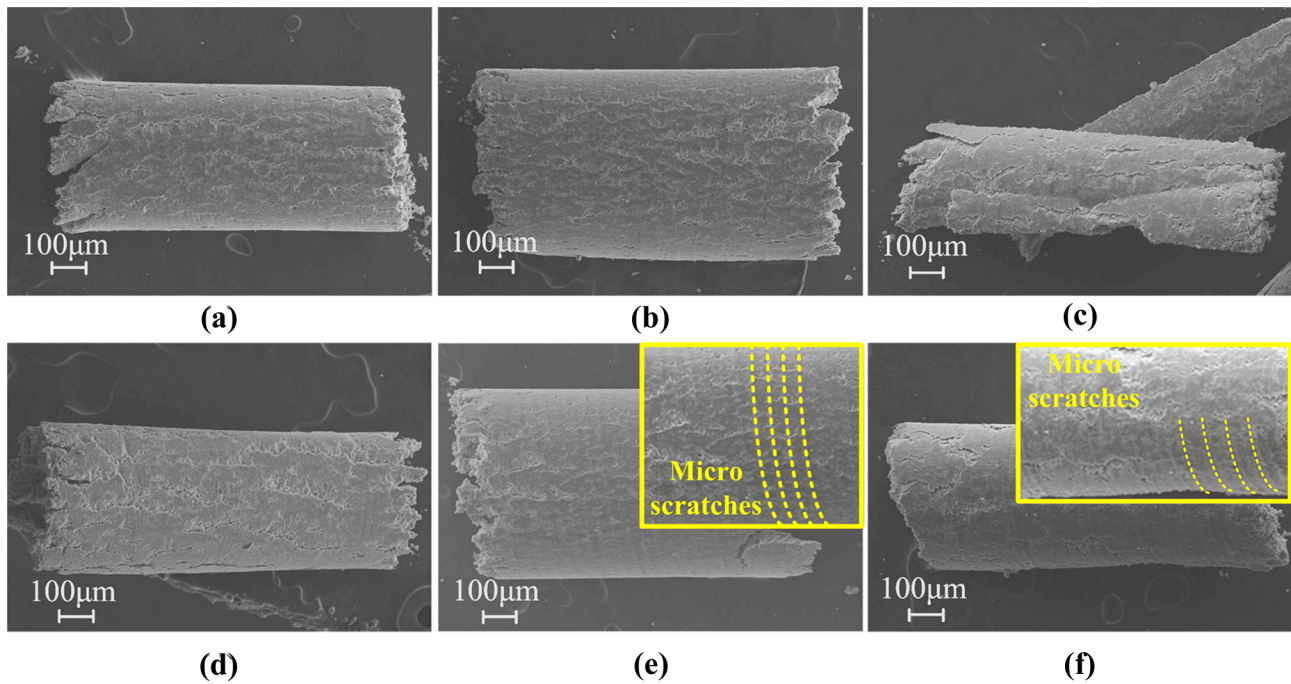


Fig. 7 SEM images of chips generated during the cutting process of non-textured tools and micro-textured tools. Chips produced by (a) T-1 tool, (b) T-2 tool, (c) T-3 tool, (d) T-4 tool, (e) T-5 tool, and (f) T-6 tool

during the cutting process, and the chips are not easily broken. The most obvious secondary cutting phenomenon is in Fig. 7e, f. It is further explained that adjusting the texture spacing can achieve the required cutting effect.

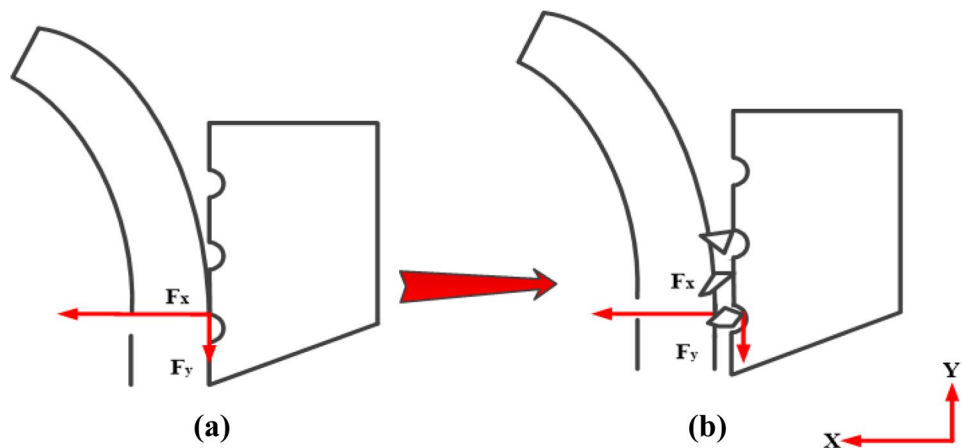
Due to the particularity of the SiCp/Al composite, the secondary cutting process could be divided into two cases, as showed in Fig. 8. In the first case, the micro-texture pits are not blocked, so the micro-texture will directly interact with the chips during the cutting process. Then some of the pits will be blocked, which greatly reduces the effect of the pits. In the second case, some broken particles and particles remaining on the chip surface may interact with the

tool surface or the pit texture. This reduces the tool surface adhesion and tool-chip contact length. Since the second case works differently from the first case, the reduction in contact length should be due to the simultaneous action of these two stages. However, due to the property of the material, the second stage could play a major role.

3.3 Cutting force

Cutting force is the main factor affecting tool wear. In the experiment, the machining direction is set as the direction of main cutting force, and its values are averaged after

Fig. 8 Schematic diagram of secondary cutting of SiCp/Al composite with micro-textured tool. (a) Initial stage of secondary cutting. (b) Stable stage of secondary cutting



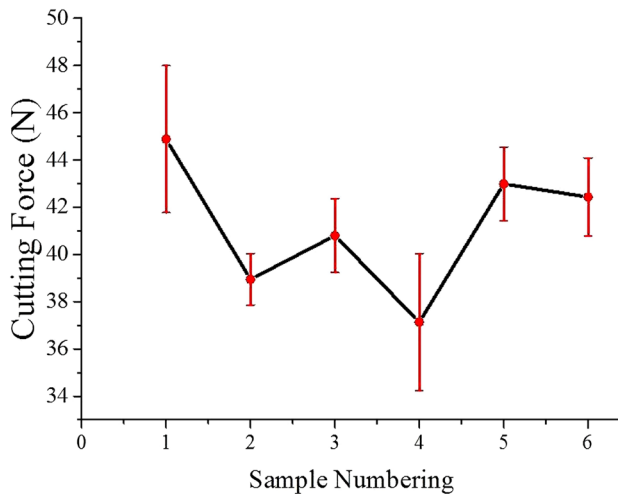


Fig. 9 The average value of the main cutting force during the cutting process of the non-textured tool and the micro-textured tool. Numbering 1–6 represents the cutting force generated by the T-1 to T-6 tools

ten times cuttings. The results are shown in Fig. 9. It is seen that T-2 to T-6 tools produce smaller cutting forces than T-1 tool. The micro-textured tool reduces the friction between the tool and the chip during the machining, thereby reducing the cutting force. With the decrease in the micro-texture spacing, the cutting force of the micro-textured tool is reduced by 13%, 9%, 17%, 4%, and 5%, respectively. The cutting forces of T-5 and T-6 tools are not reduced significantly due to the secondary cutting

during the cutting process. In the cutting process, for the T-3 tool, it is easy to break chips. Observing the chip morphology produced by T-2 and T-4 tools, one can evaluate that these two micro-textured tools are more stable during the cutting process, which will result in a significant reduction in cutting force. From the results of chip shape and cutting force, the texture spacing will influence the contact state of the sticking area, further reduce the cutting force. The SiC particle, pit, and chip may form a three-body friction for the reducing cutting force.

3.4 Workpiece surface test

Figure 10 presents the SEM images of the surface of the workpiece after cutting. It can be seen that the surfaces machined by the micro-textured tools are generally smooth and have a few cracks relatively (Fig. 10b, c, e, f). In the following, it will be shown that the residual SiC particles on the machining surface of micro-textured tools are much less than non-textured tool, and part of the SiC particles remain in the pit and interact with the chips during the cutting process.

3.5 Surface roughness

Surface roughness is an important criterion for measuring the quality of workpiece machining. The measurement method is contact measurement. Five different positions are

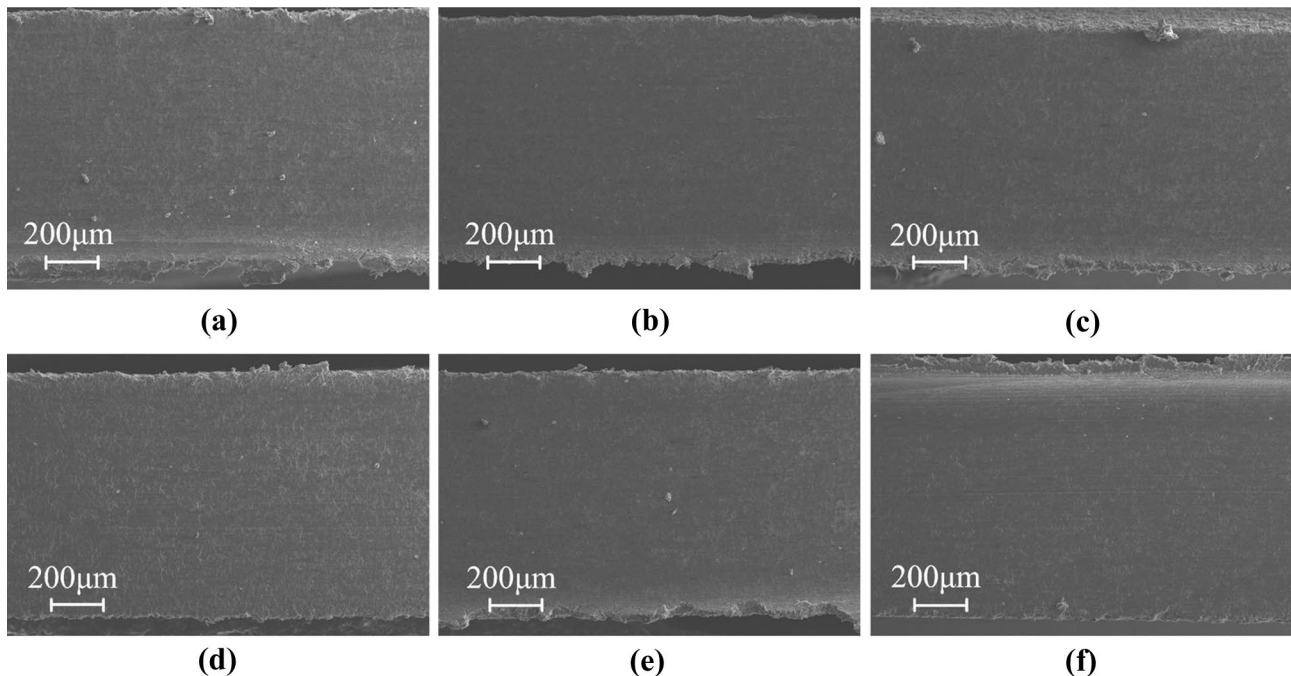


Fig. 10 SEM images of non-textured tool and micro-textured tool surface: (a) W-1, (b) W-2, (c) W-3, (d) W-4, (e) W-5, and (f) W-6

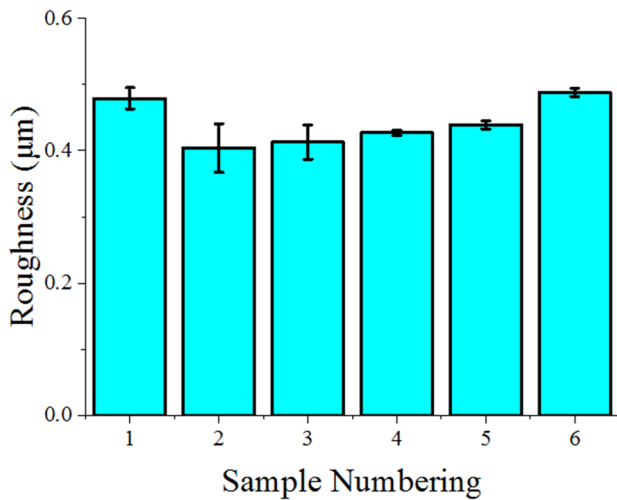


Fig. 11 Surface roughness of workpieces machined by non-textured tool and micro-textured tools. (a) W-1, (b) W-2, (c) W-3, (d) W-4, (e) W-5, and (f) W-6

selected on the surface of the workpiece for measurement, and the results are averaged. Figure 11 shows the Ra values of surface roughness workpieces W-1 to W-6. Ra is the arithmetic average of the absolute value of the contour deviation along the measurement direction and the distance from the center line, and can be used to evaluate the smoothness of machined parts. It can be seen that the surface roughness of W-1 workpieces is relatively large, and smaller for W-2 to W-6, which is consistent with the observation of the surface micro-topography (Fig. 10). Because the micro-pit texture

of the tool can collect some SiC particles, the interaction between the tool, SiC particles, and the surface of the workpiece is reduced. The surface roughness is reduced. With the decrease of the texture spacing, the secondary cutting effect produced by the texture and chip surface is more obvious. The surface will produce greater concentrated stress, and the surface roughness will become worse.

3.6 Residual stress

The residual stress of the machined workpiece is measured by a residual stress measuring instrument, which receives the signal of the machined metal surface and calculates the surface stress through the Bragg's law. Since the stress of the SiC particles in the SiCp/Al composite material cannot be measured, so the stress distribution of the aluminum matrix in the SiCp/Al composite material is measured instead. It can be seen from the results that the textured tool has a certain influence on the residual stress of the machined surface. It can be seen from Fig. 12 that this detection plan is to select 5 points on the surface of the workpiece with an interval of 0.25 cm, the position of the leftmost point is 0 cm, and the position of the rightmost point is 1 cm. It can be seen that when the texture spacing is 60–100 μm , the residual stress on the machined surface of the workpiece is smaller than that of a non-textured tool but when the spacing is 20–40 μm , the residual stress on the machined surface of the workpiece tends to increase. It can be observed from the surface of the chip that the secondary cutting phenomenon is the most serious when the texture spacing is 20–40 μm .

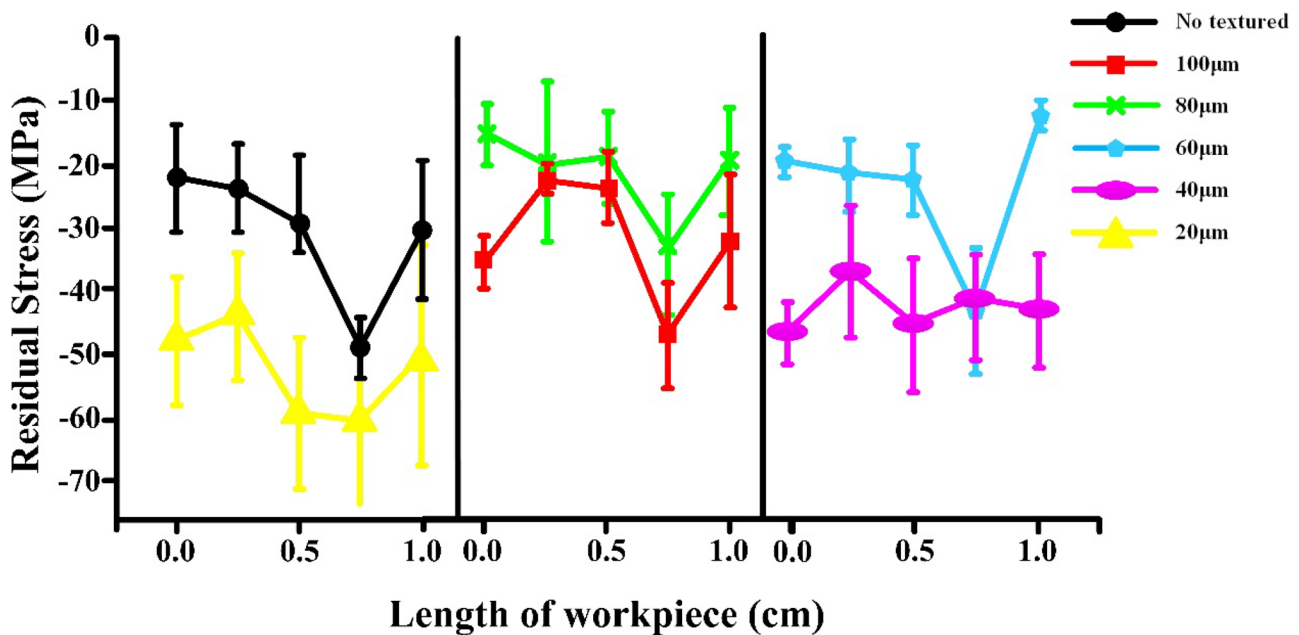


Fig. 12 Surface residual stress of workpieces machined by non-textured tools and micro-textured tools

With the spacing decrease, the contact state of the sticking area will change; the stress between the tool and the chip becomes larger, which increases the machined surface residual stress of the workpiece.

4 Conclusion

In this paper, a micro-pit array textured tool with a diameter of 5 μm is applied to the machining of SiCp/Al composite. Micro-textured tools can not only improve the cutting performance of the tool, but also improve the surface quality of the workpiece. Considering the cutting performance and surface quality, the T-5 tool shows better tool properties. The conclusions are the following:

1. Serious tool wear and adhesion occurred during dry cutting SiCp/Al composite; however, by using micro-textured tools, they can be reduced significantly. It is attributed to the interaction between the micro-pit, SiC particles, and the chips.
2. The contact length between the tool and the chip in the non-texture case is the largest during the cutting process. The micro-textured tools can reduce the contact length through the micro pits.
3. Micro-textured tools produce secondary cutting during cutting process. Increasing the pit spacing of micro-textured tool can reduce the impact of secondary cutting. Main cutting force is reduced by use of micro-texture. The cutting force is reduced largest by 17% in the case of the tool with spacing 60 μm (T-4). Spacing 40 μm is a turning point for anti-adhesion. The texture anti-adhesion becomes worse when the spacing exceeds or is less than 40 μm .
4. The micro-pits texture can collect SiC particles, which reduces the number of residual particles on the surface of the workpiece, as well as the interaction between SiC particles, tool, and workpiece for improving the surface quality. This interaction is enhanced with the decreasing texture spacing, which causes greater concentrated stress on the chip surface, further aggravates the secondary cutting phenomenon. However, too small texture spacing could change the contact state of the sticking area, causing greater residual stress on the workpiece's surface. Focusing on the tool life, T-5 shows the best cutting performance.

Author contribution V.L. Popov and Xu Wang designed the experimental plan, and Zhanjiang Yu and Jinkai Xu designed and adjusted the experiment set-up. The measurement was performed by Jinkai Xu, Yiquan Li, and Xu Wang. V.L. Popov and Zhanjiang Yu processed and analyzed the experimental data. Huadong Yu supervised the project and the collaboration.

Funding Open Access funding enabled and organized by Projekt DEAL. This work was supported by the National Key Research and Development Plan Project (No. 2018YFB1107403), the “111” Project of China (No. D17017), Jilin Province Scientific and Technological Development Program (No. 20190101005JH, No. 20180201057GX, No. 20190302076GX), and Science Fund for Youth Scholar of Changchun University of Science Technology (No. XQNJJ-2018–09).

Availability of data and materials The data that support the findings of this study are available from the corresponding author upon reasonable request.

Declarations

Ethical approval Not applicable.

Consent to participate Not applicable.

Consent to publish Not applicable.

Competing interests The authors declare no competing interests.

Open Access This article is licensed under a Creative Commons Attribution 4.0 International License, which permits use, sharing, adaptation, distribution and reproduction in any medium or format, as long as you give appropriate credit to the original author(s) and the source, provide a link to the Creative Commons licence, and indicate if changes were made. The images or other third party material in this article are included in the article's Creative Commons licence, unless indicated otherwise in a credit line to the material. If material is not included in the article's Creative Commons licence and your intended use is not permitted by statutory regulation or exceeds the permitted use, you will need to obtain permission directly from the copyright holder. To view a copy of this licence, visit <http://creativecommons.org/licenses/by/4.0/>.

References

1. Muthukrishnan N, Murugan M, Rao KP (2008) Machinability issues in turning of Al-SiC (10p) metal matrix composites. *Int J Adv Manuf Syst* 39(3–4):211–218
2. Goo BC (2016) Al/SiCp brake discs produced by dissimilar cast-bonding. *Mater Manuf Process* 31(10):1318–1323
3. Hong SJ, Kim HM, Huh D, Suryanarayana C, Chun BS (2003) Effect of clustering on the mechanical properties of SiC particulate-reinforced aluminum alloy 2024 metal matrix composites. *Mater Sci Eng A* 347(1–2):198–204
4. Tosun G (2011) Statistical analysis of process parameters in drilling of Al/SiCp metal matrix composite[J]. *Int J Adv Manuf Technol* 55(5–8):477–485
5. Zhou M, Wang M, Dong GJ (2015) Experimental investigation on rotary ultrasonic face grinding of SiCp/Al composites. *Mater Manuf Process* 31(5):673–678
6. John R, Lin R, Jayaraman K, Bhattacharyya D (2020) Effects of machining parameters on surface quality of composites reinforced with natural fibers. *Mater Manuf Process* 36(2):73–78
7. Liu JW, Cheng K, Ding H, Chen SJ, Zhao L (2018) Simulation study of the influence of cutting speed and tool-particle interaction location on surface formation mechanism in micromachining SiCp/Al composites. *Proc IMechE Part C: J Mech Eng Sci* 232(11):2044–2056

8. Niu ZC, Cheng K (2019) An experimental investigation on surface generation in ultraprecision machining of particle reinforced metal matrix composites. *Int J Adv Manuf Technol* 105:4499–4507
9. Seeman M, Ganesan G, Karthikeyan R, Vealyudham A (2010) Study on tool wear and surface roughness in machining of particulate aluminum metal matrix composite-response surface methodology approach. *Int J Adv Manuf Technol* 48(5–8):613–624
10. Liu Y, Deng J, Wang W, Duan R, Meng R, Ge D, Li X (2018) Effect of texture parameters on cutting performance of flank-faced textured carbide tools in dry cutting of green Al₂O₃ ceramics. *Ceram Int* 44(11):13205–13217
11. Zhang GL, Deng JX, Ge DL, Wang W, Zhang X, Liu YY (2018) Effect of sine-type surface macrotexture on tribological property of carbide. *Tool Eng* 52(2):12–17
12. Wu Z, Bao H, Liu L, Xing YQ, Huang P, Zhao GL (2020) Numerical investigation of the performance of micro-textured cutting tools in cutting of Ti-6Al-4V alloys. *Int J Adv Manuf Technol* 108(10):463–474
13. Zheng KR, Yang FZ, Zhang N, Liu QY, Jiang FL (2020) Study on the cutting performance of micro textured tools on cutting Ti-6Al-4V Titanium Alloy. *Micromachines* 11:137
14. Feng YH, Zhang JY, Wang L, Zhang WQ, Dong YP (2019) Study on secondary cutting phenomenon of micro-textured self-lubricating ceramic cutting tools with different morphology parameters formed via in situ forming of Al₂O₃-TiC. *Int J Adv Manuf Technol* 104:3821–3833
15. Feng YH, Yuan PD, Wang L, Zhang JY, Zhang JH, Zhou X (2020) Experimental investigation of different morphology textured ceramic tools by in-situ formed for the dry cutting. *Int J Appl Ceram Technol* 17:1108–1118
16. Vasumathy D, Meena A (2017) Influence of micro scale textured tools on tribological properties at tool-chip interface in turning AISI 316 austenitic stainless steel. *Wear* 376–377:1747–1758
17. Xing YQ, Deng JX, Feng XT, Yu S (2013) Effect of laser surface texturing on Si₃N₄/TiC ceramic sliding against steel under dry friction. *Mater Des* 52:234–245
18. Xing YQ, Deng JX, Wang XS, Ehmann K, Cao J (2016) Experimental assessment of laser textured cutting tools in dry cutting of aluminum alloys. *J Manuf Sci Eng* 138(7):071006
19. Parida AK, Rao PV, Ghosh S (2020) Performance of textured tool in turning of Ti-6Al-4V alloy: numerical analysis and experimental validation. *J Braz Soc Mech Sci Eng* 42(5):715–725
20. Sivaiah P, Muralidhar SM, Venkatesu S, Yoganjaneyulu G (2020) Investigation on turning process performance using hybrid-textured tools under dry and conventional cooling environment. *Mater Manuf Process* 35(16):1852–1859
21. Elias JV, Prasanna VN, Deepak LK, Jose M (2021) Tool texturing for micro-turning applications — an approach using mechanical micro indentation. *Mater Manuf Process* 36(1):84–93
22. Dandekar CR, Shin YC (2009) Multi-step 3-D finite element modeling of subsurface damage in machining particulate reinforced metal matrix composites. *Compos - A: Appl Sci Manuf* 40(8):1231–1239
23. Tang DW, Zhang WM, Zhao RL, Lv XJ (2017) Machining of SiCp/Al composites: effect of tool corner radius on residual stresses, cutting force and temperature. *Adv Mat Res* 1142:265–270

Publisher's Note Springer Nature remains neutral with regard to jurisdictional claims in published maps and institutional affiliations.